Electronic Supplementary Material (ESI) for Physical Chemistry Chemical Physics.
This journal is © the Owner Societies 2018

Supplementary Information

Interfacing Tetrapyridyl-C_{60} with Porphyrin Dimers *via π*-Conjugated Bridges: Artificial Photosynthetic Systems with Ultrafast Charge Separation

Christina Stangel,[a],[b],‡ Fabian Plass,[c],‡ Asterios Charisiadis,[a] Emmanouil Giannoudis,[a] Georgios Chararalambidis,[a] Kostas Karikis,[a] Georgios Rotas,[b] Galateia E. Zervaki,[a] Nektarios N. Lathiotakis,[b] Nikos Tagmatarchis,[b] Axel Kahnt,*[c],[d] and Athanassios G. Coutsolelos*[a]*

[a] Laboratory of Bioinorganic Chemistry, Department of Chemistry, University of Crete, Voutes Campus, 70013 Heraklion, Crete, Greece. E-mail: acoutsol@uoc.gr

[b] Theoretical and Physical Chemistry Institute, National Hellenic Research Foundation, 48 Vassileos Constantinou Avenue, Athens11635, Greece. E-mail: tagmatar@eie.gr

[c] Chair of Physical Chemistry I, Department of Chemistry and Pharmacy, Friedrich-Alexander University, Erlangen-Nürnberg (FAU), Egerlandstr. 3, 91058 Erlangen, Germany

[d] Leibniz Institute of Surface Engineering (IOM), Permoserstrasse 15, 04318 Leipzig, Germany. E-mail: axel.kahnt@iom-leipzig.de

‡These authors have equally contributed.

Contents

Fig. S1 ^{1}H NMR spectrum of compound **3**.	**S3**
Fig. S2 ^{13}C NMR spectrum of compound **3**.	**S3**
Fig. S3 ^{1}H NMR spectrum of compound **5**.	**S4**
Fig. S4 ^{13}C NMR spectrum of compound **5**.	**S4**
Fig. S5 ^{1}H NMR spectrum of compound **6**.	**S5**
Fig. S6 ^{13}C NMR spectrum of compound **6**.	**S5**
Fig. S7 ^{1}H NMR spectrum of compound **7**.	**S6**
Fig. S8 ^{13}C NMR spectrum of compound **7**.	**S6**
Fig. S9 ^{1}H NMR spectrum of **C_{60}-tpyr**.	**S7**
Fig. S10 ^{13}C NMR spectrum of **C_{60}-tpyr**.	**S7**
Fig. S11 Different views of the optimized structure of **C_{60}-tpyr•[(ZnP)$_2$]$_2$**.	**S8**
Fig. S12 Calculated absorption spectrum of **C_{60}-tpyr•[(ZnP)$_2$]$_2$** (top) and the orbital distribution corresponding to all the molecular orbitals that are involved in the strong optical excitation at 435 nm (bottom).	**S8**
Fig. S13 Steady state absorption spectra of toluene solutions containing 1 x 10^{-6} **M C_{60}-tpyr** and 0 – 4 x 10^{-6} M **(ZnP)$_2$**.	**S9**
Fig. S14 Job plots of **C_{60}-tpyr•(ZnP$_2$)$_2$** in anisole.	**S10**
Fig. S15 Steady state absorption spectra of toluene solutions containing 1 x 10^{-6} **M C_{60}-tpyr** and 0 – 1 x 10^{-5} M **ZnP**.	**S11**
Fig. S16 Fluorescence spectra of **C_{60}-tpyr•(ZnP)$_4$** in toluene upon photoexcitation at 430 nm containing 1 x 10^{-6} M **C_{60}-tpyr** and 0 – 1 x 10^{-5} M **ZnP**.	**S12**
Fig. S17 Nanosecond transient absorption spectra of **(ZnP)$_2$**.	**S13**
Fig. S18 Nanosecond transient absorption spectra of **C_{60}tpyr**.	**S14**
Figs S19-21 Femtosecond transient absorption spectra of **C_{60}-tpyr•[(ZnP)$_2$]$_2$** in different solvents and different **C_{60}-tpyr** and **(ZnP)$_2$** ratios.	**S15-16**
Fig. S22 Femtosecond transient absorption spectra of **C_{60}-tpyr•(ZnP)$_4$**.	**S16**
Fig. S23 Fluorescence time profiles of **C_{60}-tpyr•[(ZnP)$_2$]$_2$**.	**S17**

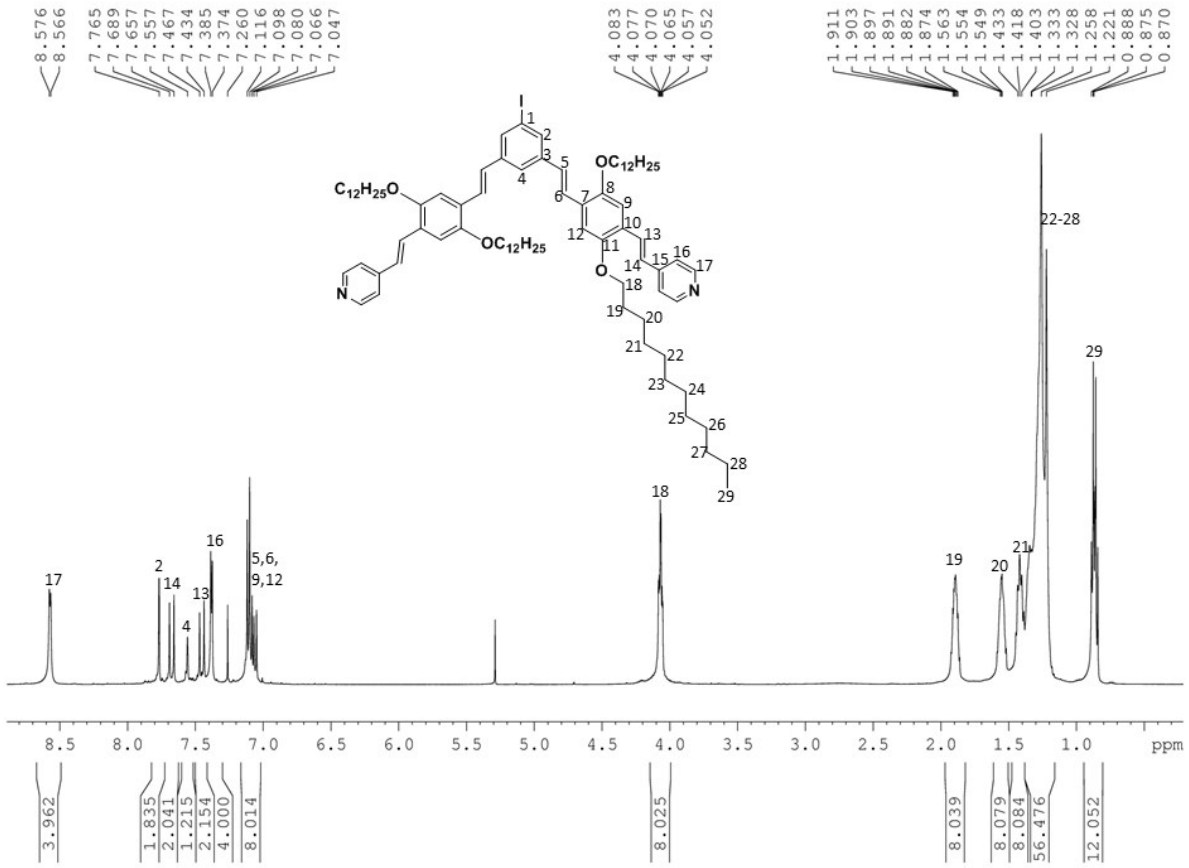

Fig. S1 ^{1}H NMR spectrum of compound **3** (500 MHz, $CDCl_3$)

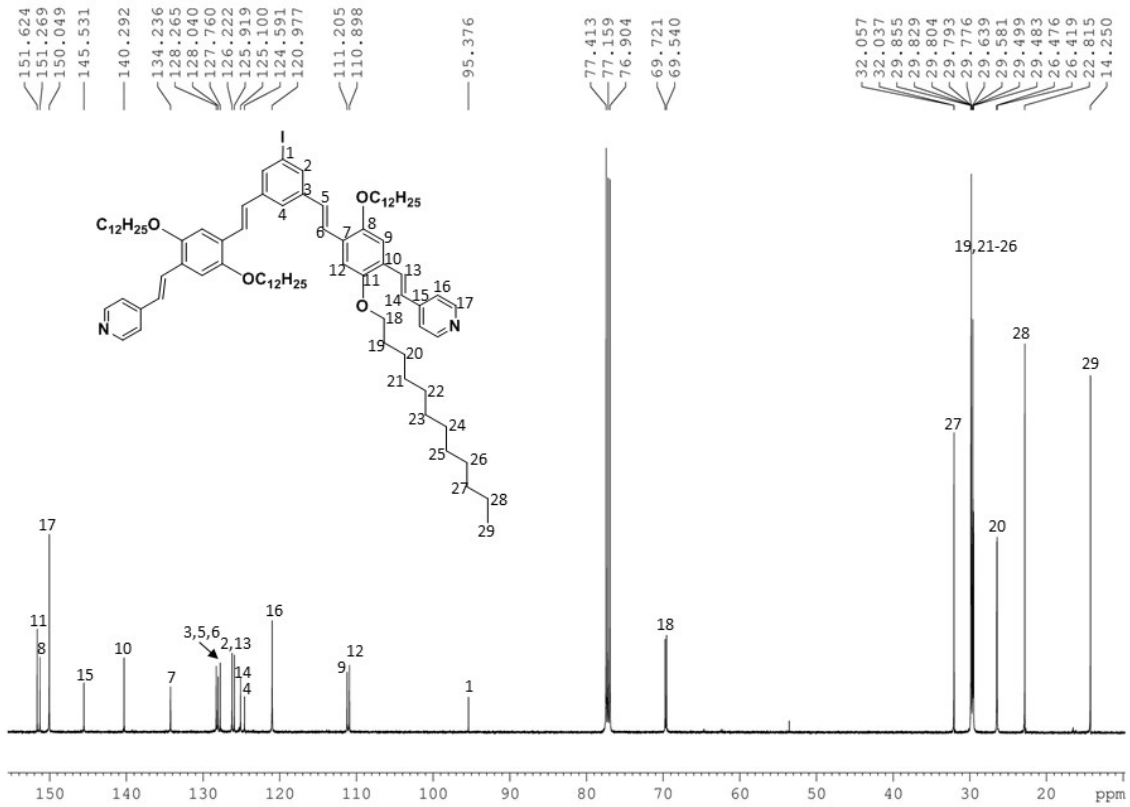

Fig. S2 ^{13}C NMR spectrum of compound **3** (125 MHz, $CDCl_3$)

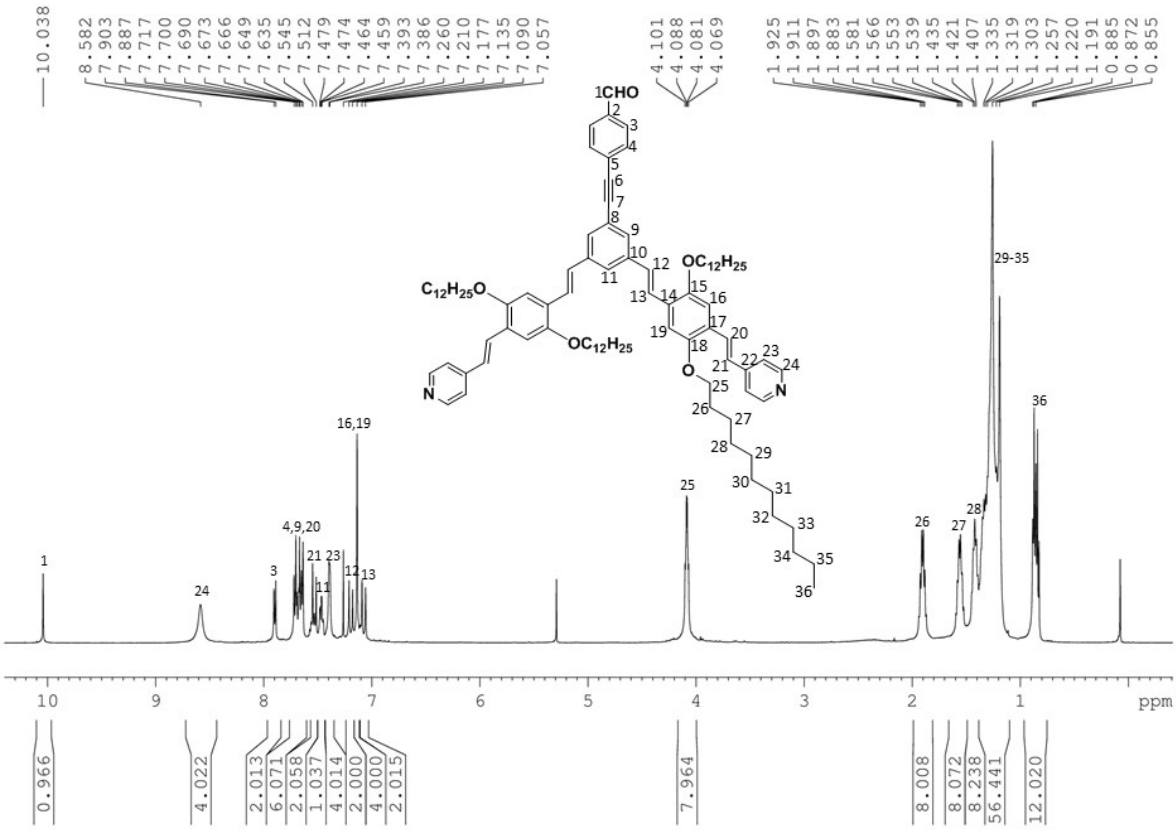

Fig. S3 ^{1}H NMR spectrum of compound **5** (500 MHz, $CDCl_3$)

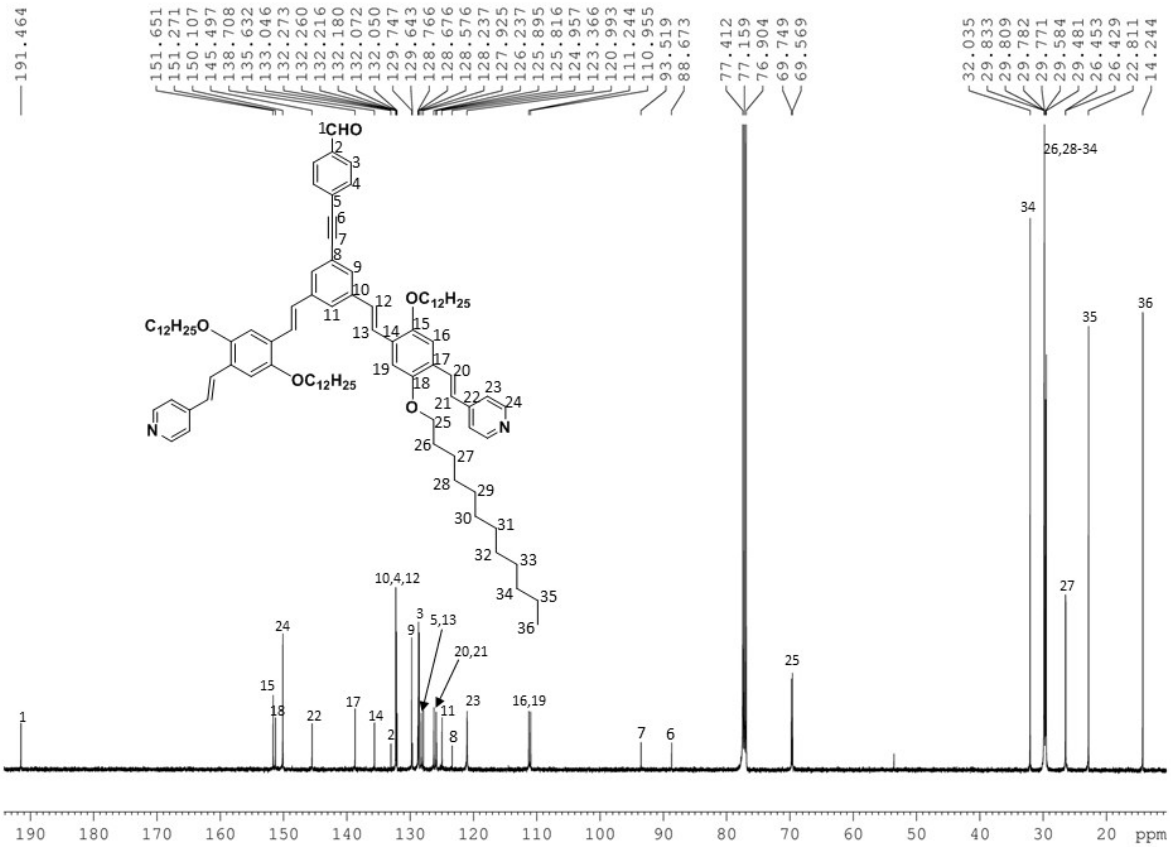

Fig. S4 ^{13}C NMR spectrum of compound **5** (125 MHz, $CDCl_3$)

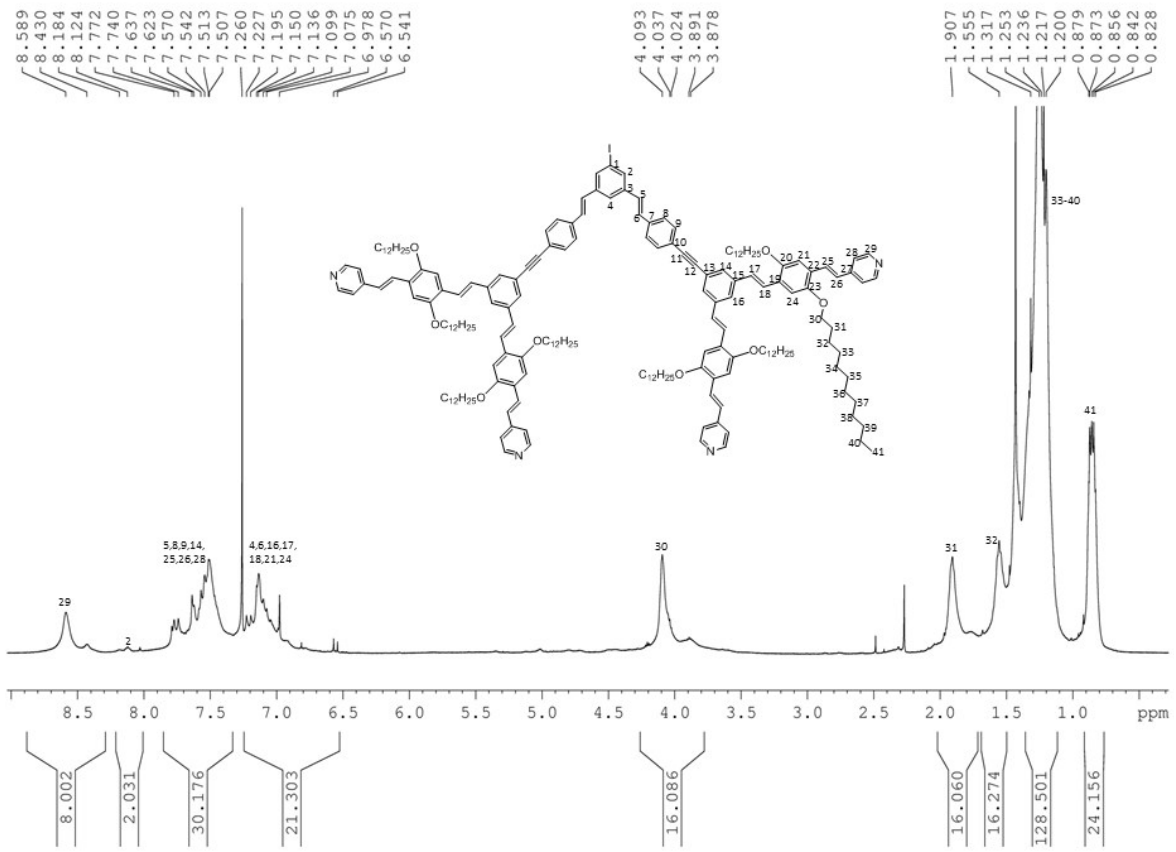

Fig. S5 ^{1}H NMR spectrum of compound **6** (500 MHz, $CDCl_3$)

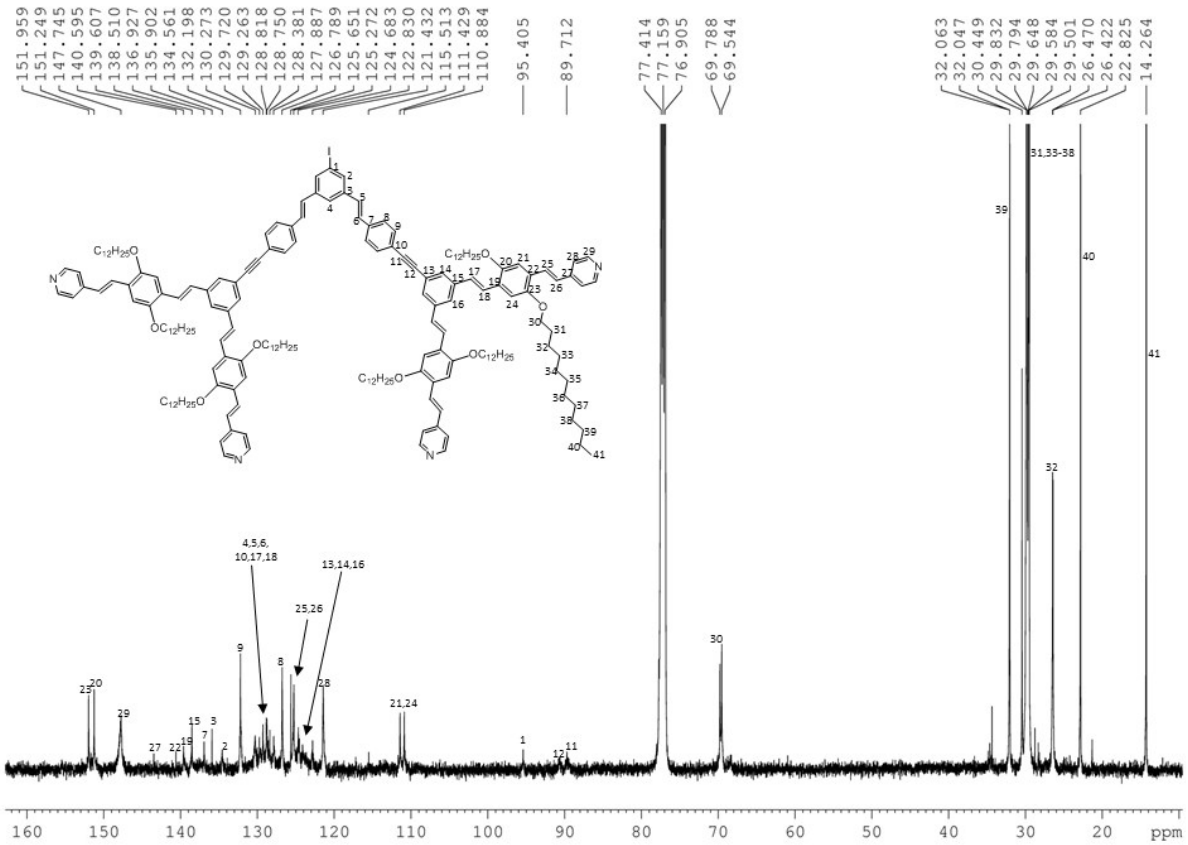

Fig. S6 ^{13}C NMR spectrum of compound **6** (125 MHz, $CDCl_3$)

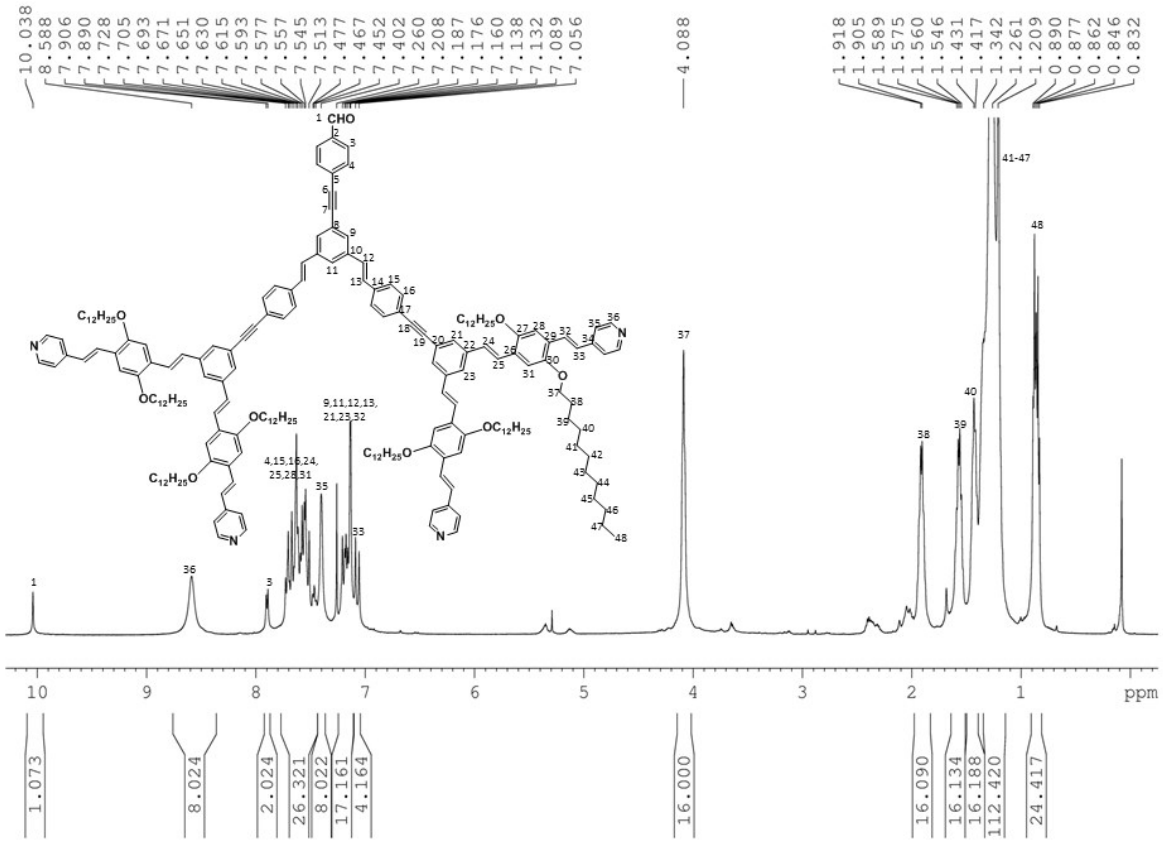

Fig. S7 ^{1}H NMR spectrum of compound **7** (500 MHz, $CDCl_3$)

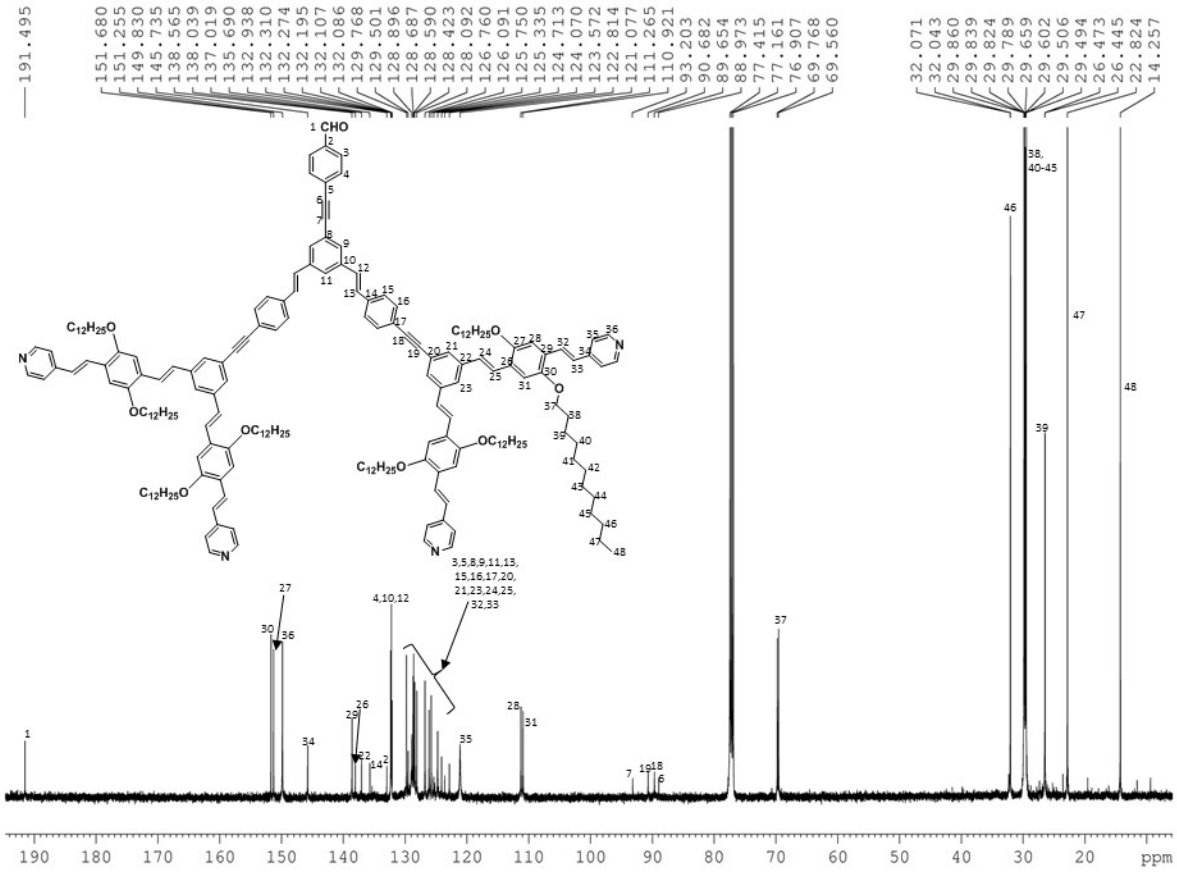

Fig. S8 ^{13}C NMR spectrum of compound **7** (125 MHz, $CDCl_3$)

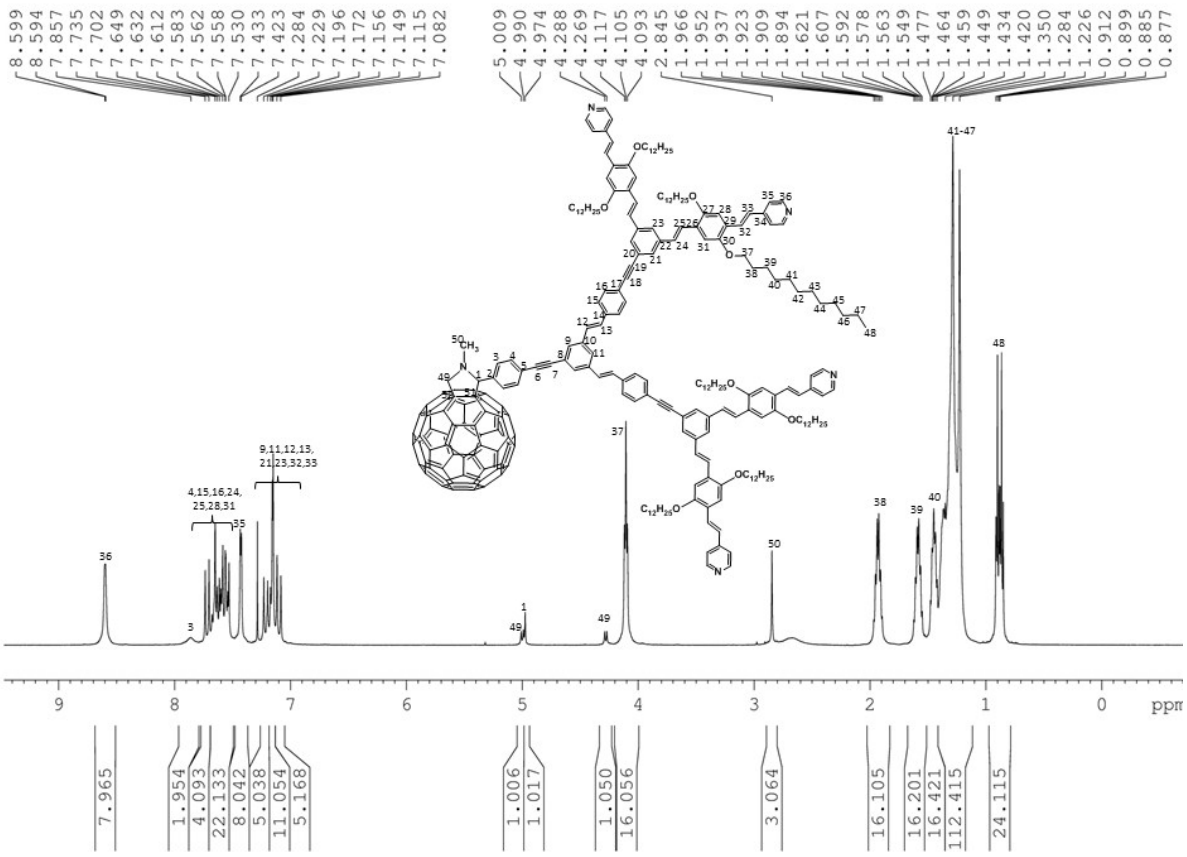

Fig. S9 ^{1}H NMR spectrum of **C_{60}-tpyr** (500 MHz, $CDCl_3$)

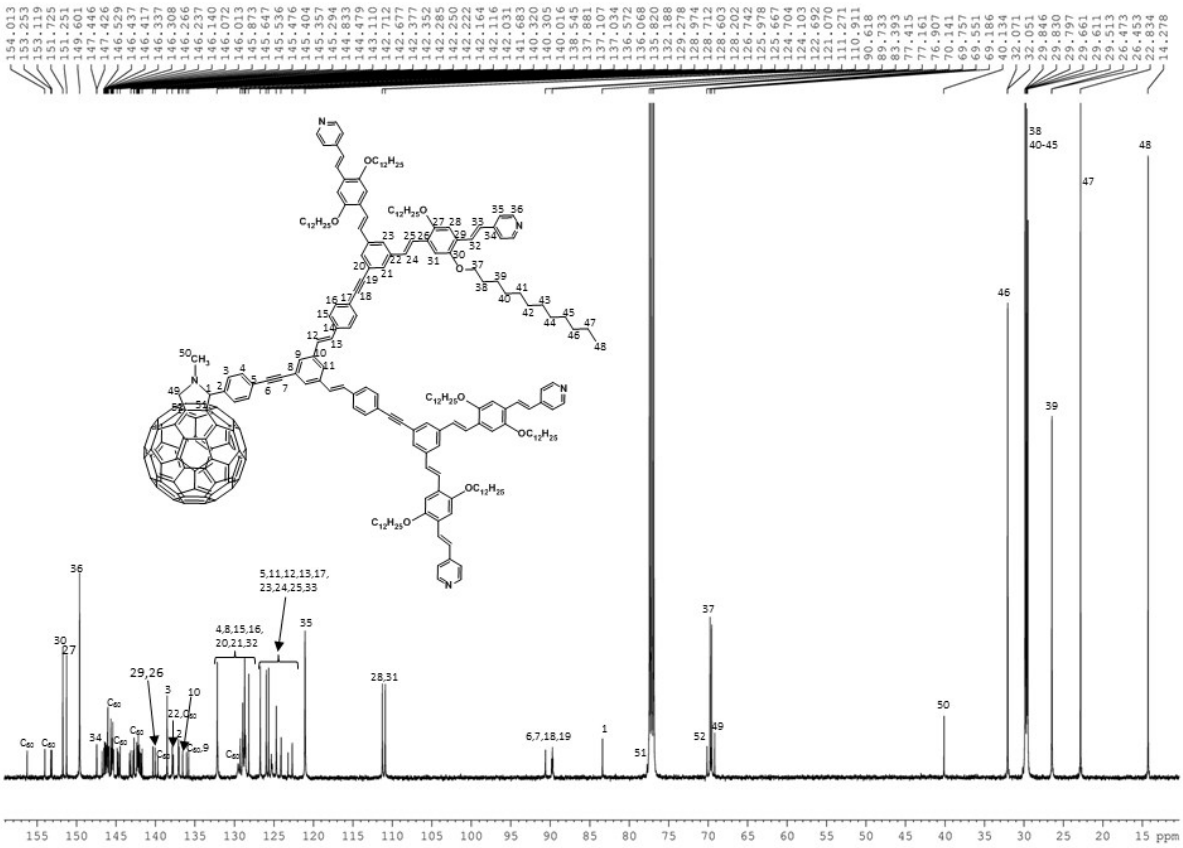

Fig. S10 ^{13}C NMR spectrum of **C_{60}-tpyr** (125 MHz, $CDCl_3$)

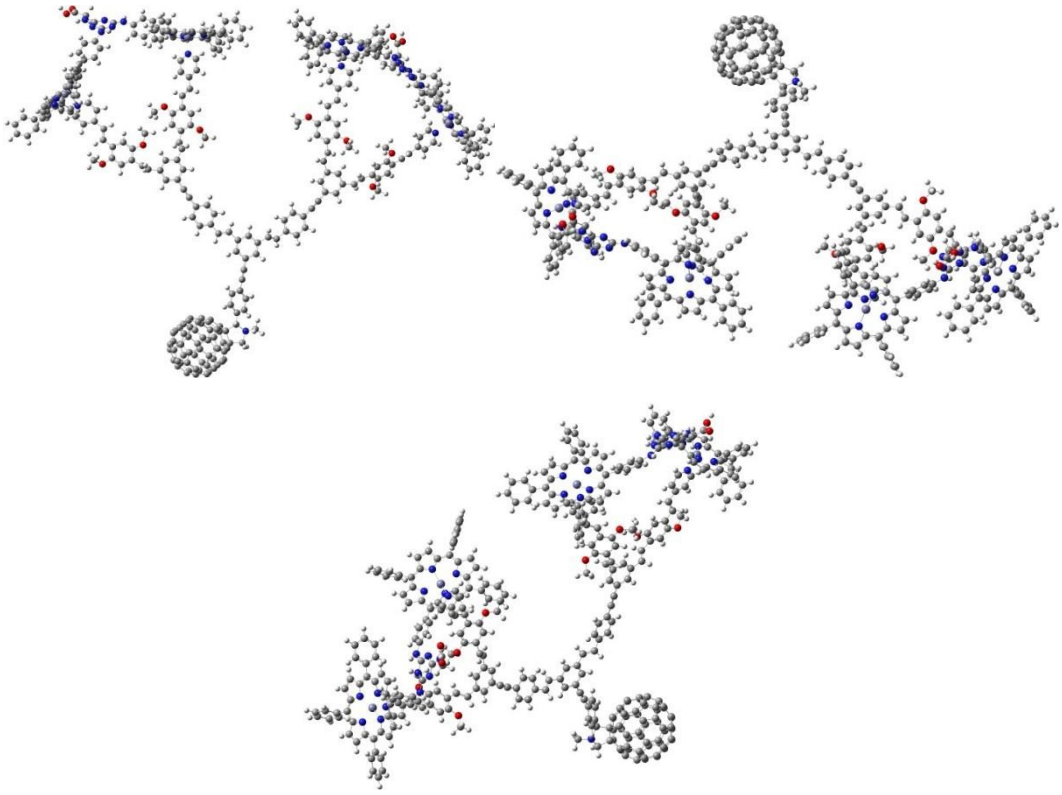

Fig. S11 Different views of the optimized structure of **C_{60}-tpyr•[(ZnP)$_2$]$_2$** using the PM6 semiempirical method.

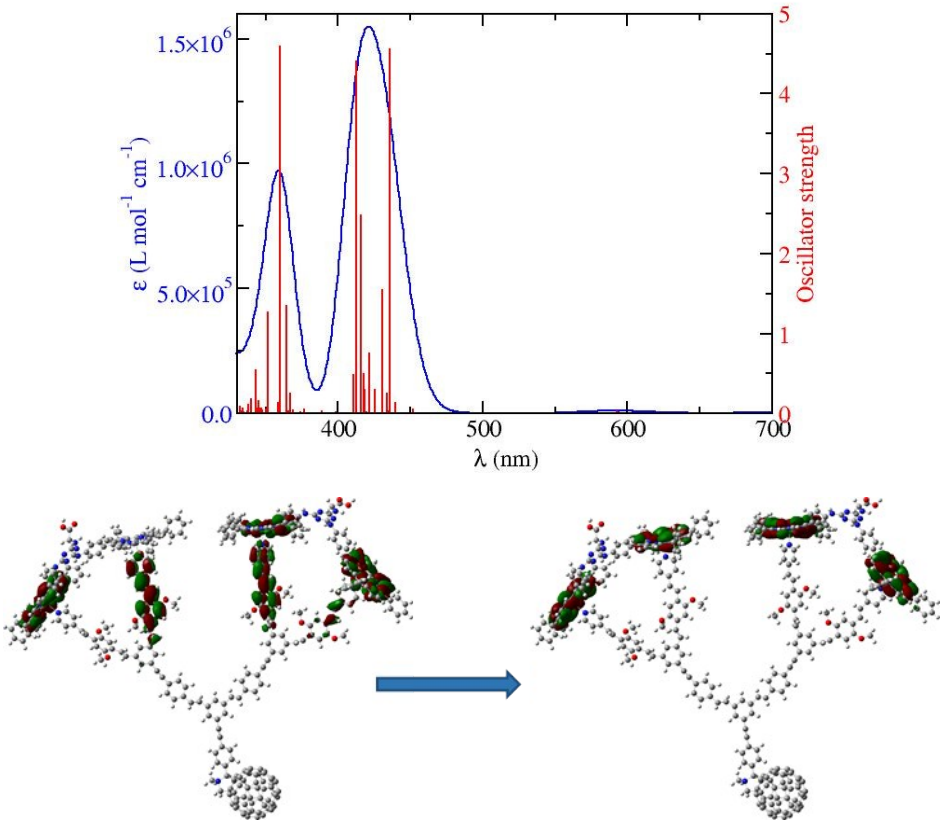

Fig. S12 Calculated absorption spectrum of **C_{60}-tpyr•[(ZnP)$_2$]$_2$** using the ZINDO method (top) and the orbital distribution corresponding to all the molecular orbitals that are involved in the strong optical excitation at 435 nm (bottom).

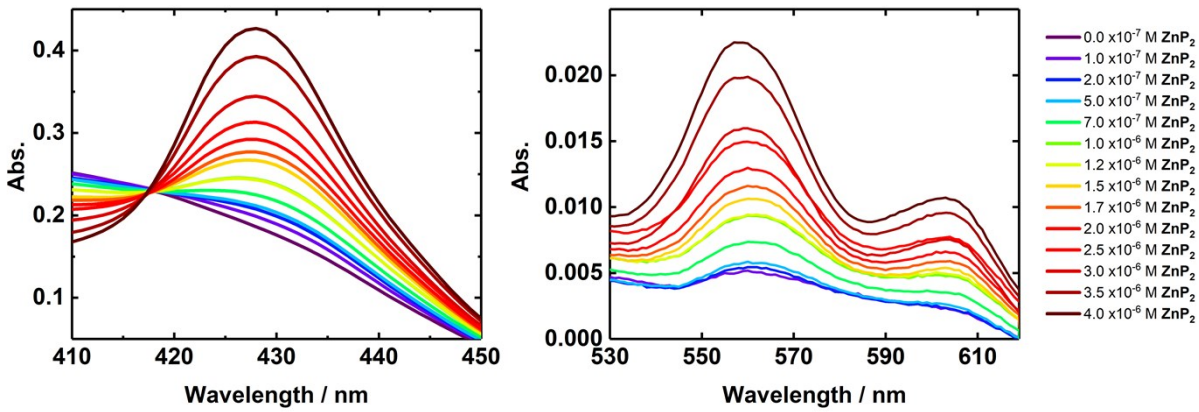

Fig. S13 Steady state absorption spectra of anisole solutions containing 1 x 10^{-6} M **C_{60}-tpyr** and 0 - 4 x 10^{-6} M **$(ZnP)_2$**. Zoom of the Soret-band (left part) and Q-bands (right part) regions.

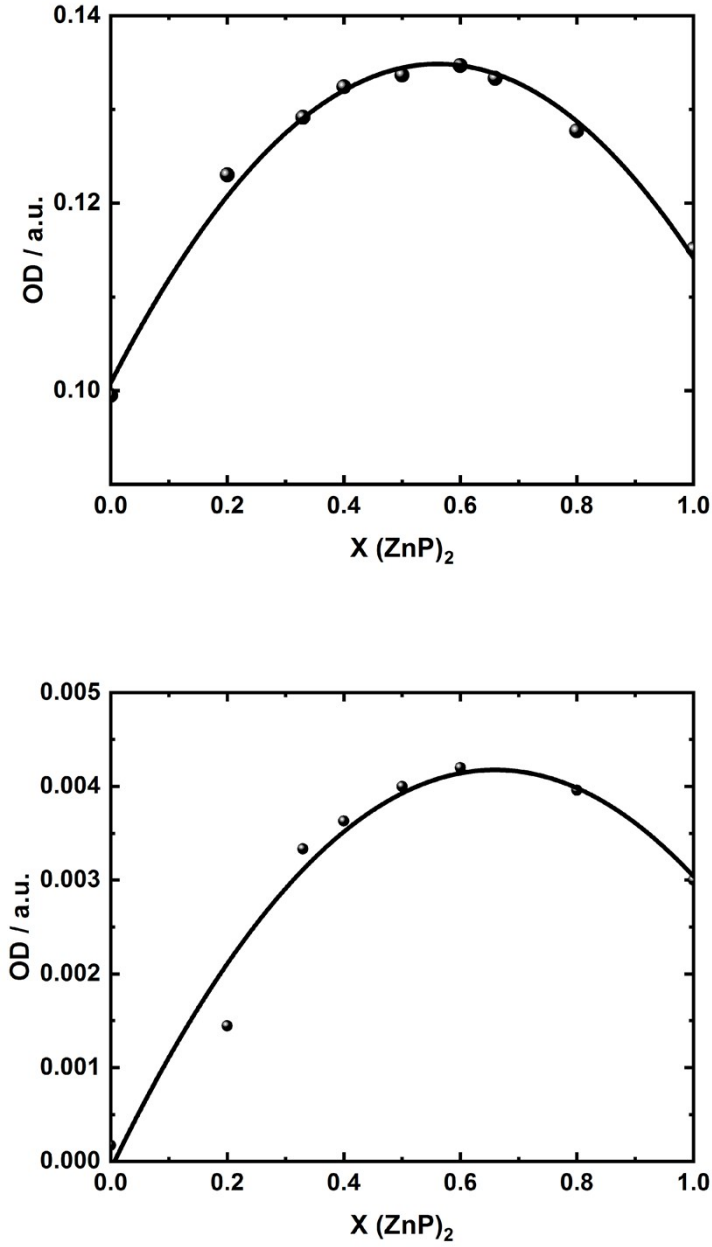

Fig. S14 Job plots of **C_{60}-tpyr•[(ZnP)$_2$]$_2$** in anisole with different mole fractions of **C_{60}-tpyr** and **(ZnP)$_2$** at 431 nm (upper figure) and 560 nm (lower figure). The jobs plots (431 nm and 560 nm) are originating from two independent measurement series.

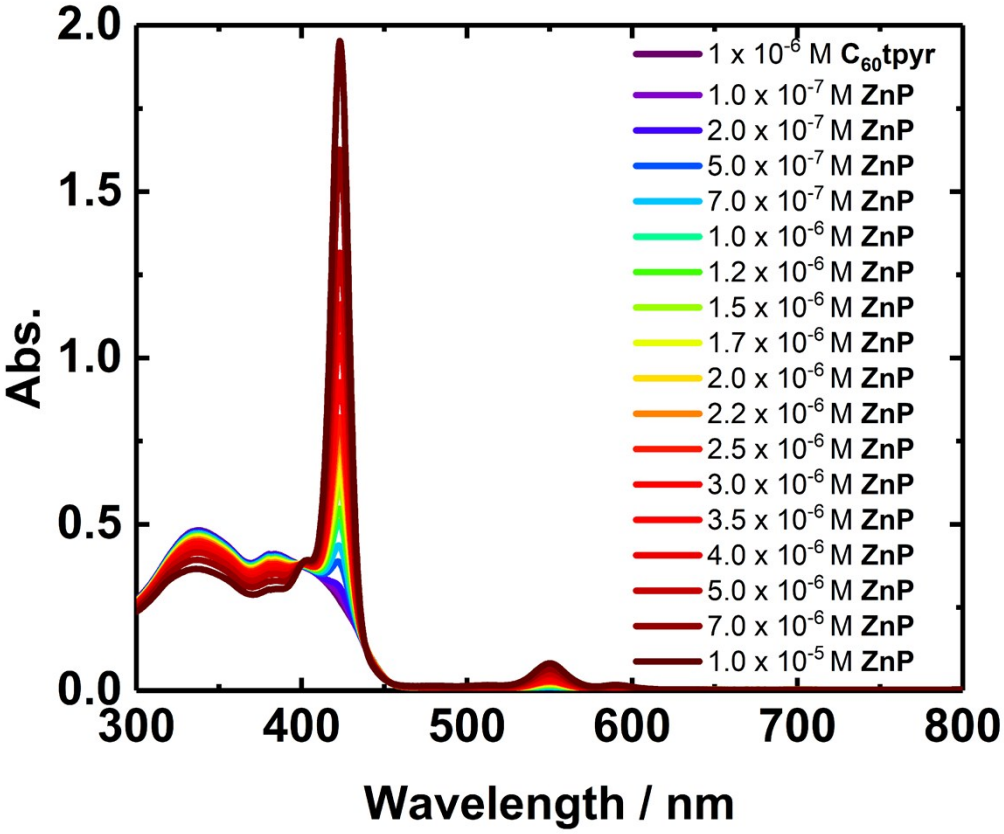

Fig. S15 Steady state absorption spectra of toluene solutions containing 1 x 10^{-6} M **C_{60}-tpyr** and 0 – 1 x 10^{-5} M **ZnP**.

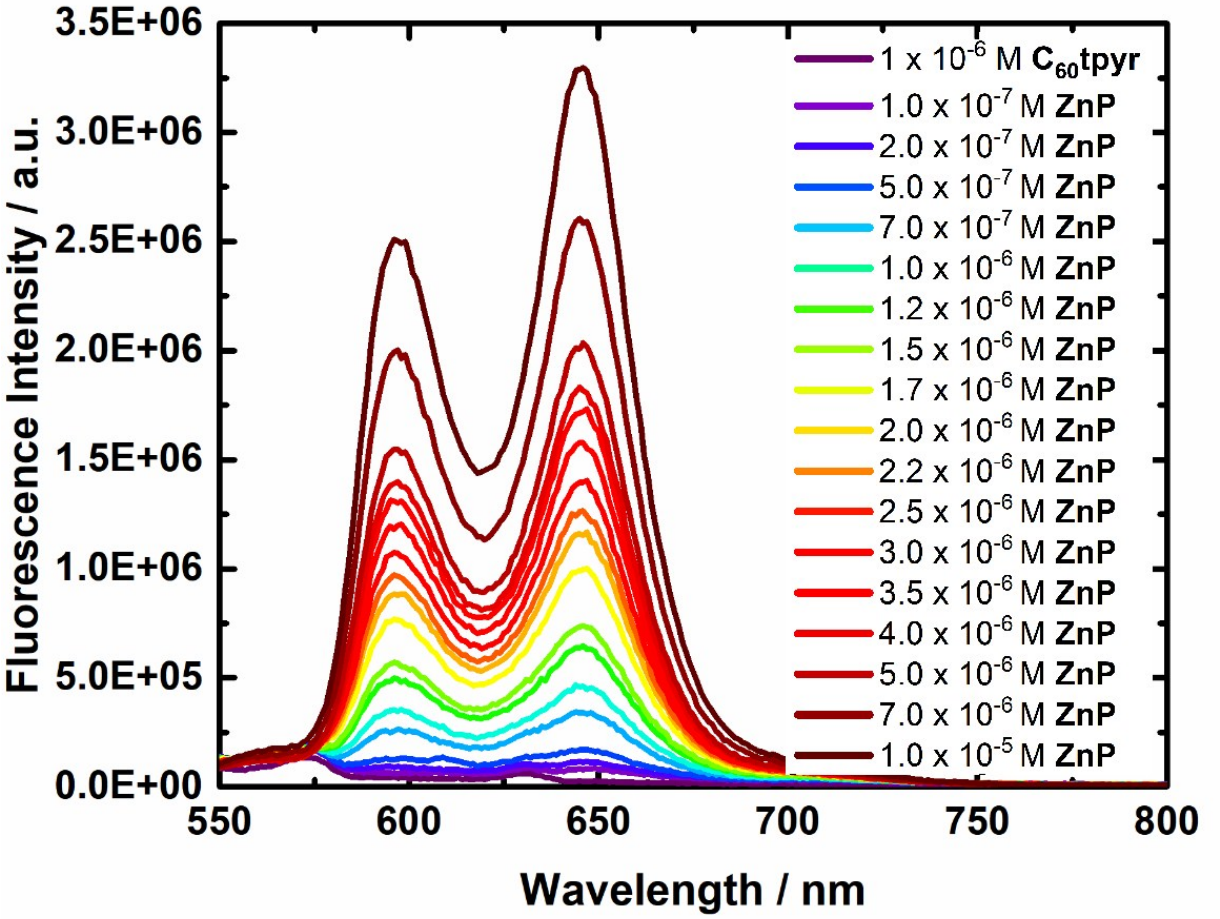

Fig. S16 Fluorescence spectra of **C_{60}-tpyr•(ZnP)$_4$** in toluene upon photoexcitation at 430 nm containing 1 x 10^{-6} M **C_{60}-tpyr** and 0 – 1 x 10^{-5} M **ZnP**.

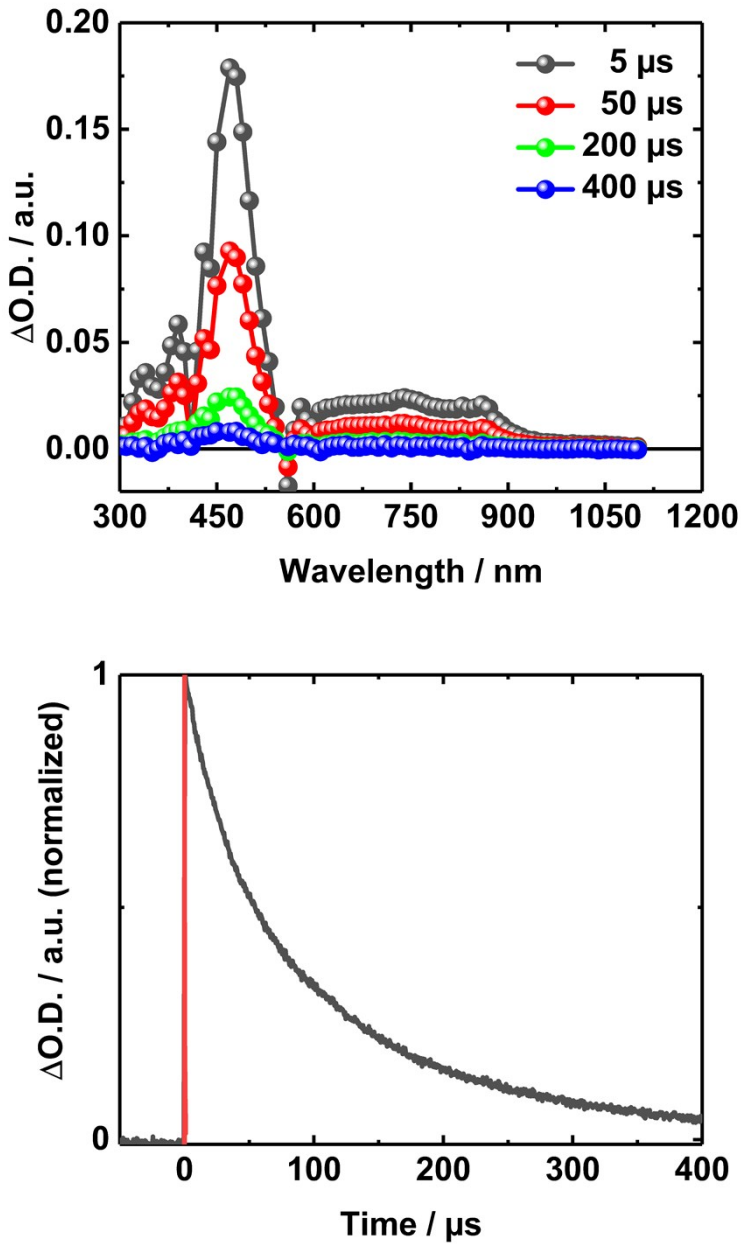

Fig. S17 Nanosecond transient absorption spectra of **(ZnP)$_2$**, obtained upon photoexcitation at 355 nm (5 ns FWHM, 10 mJ) in argon saturated toluene at different time delays (upper part) and the corresponding time-absorption profiles at 470 nm (lower part). The black time-absorption profile was measured under argon saturation, while the red time-absorption profile was measured under oxygen saturation.

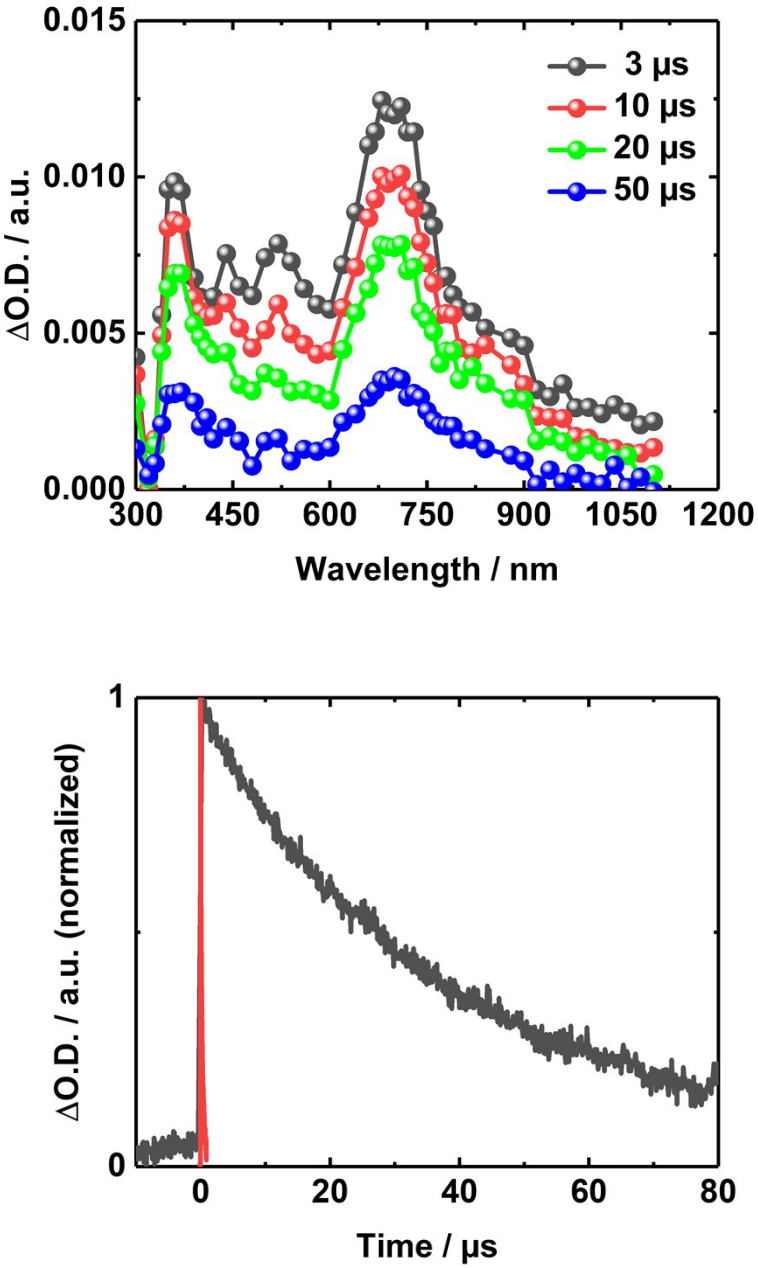

Fig. S18 Nanosecond transient absorption spectra of **C_{60}-tpyr**, obtained upon photoexcitation at 355 nm (5 ns FWHM, 10 mJ) in argon saturated toluene at different time delays (upper part) and the corresponding time-absorption profiles at 470 nm (lower part). The black time-absorption profile was measured under argon saturation, while the red time-absorption profile was measured under oxygen saturation.

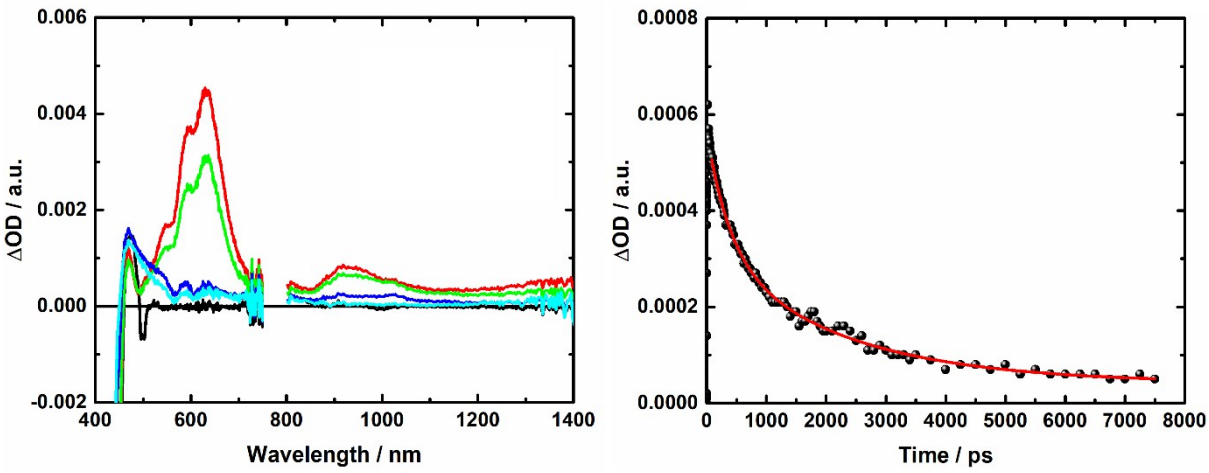

Fig. S19 Left: Femtosecond transient absorption spectra of **C_{60}-tpyr•[(ZnP)$_2$]$_2$** in argon saturated toluene containing 1 x 10^{-6} M **C_{60}-tpyr** and 1 x 10^{-6} M **(ZnP)$_2$** upon photoexcitation at 430 nm at different time delays, 1 ps (black), 10 ps (red), 100 ps (green), 1000 ps (blue) and 7500 ps (cyan). Right: Corresponding time absorption profile at 1014 nm. The solid line shows the biexponential fit of the transient absorption.

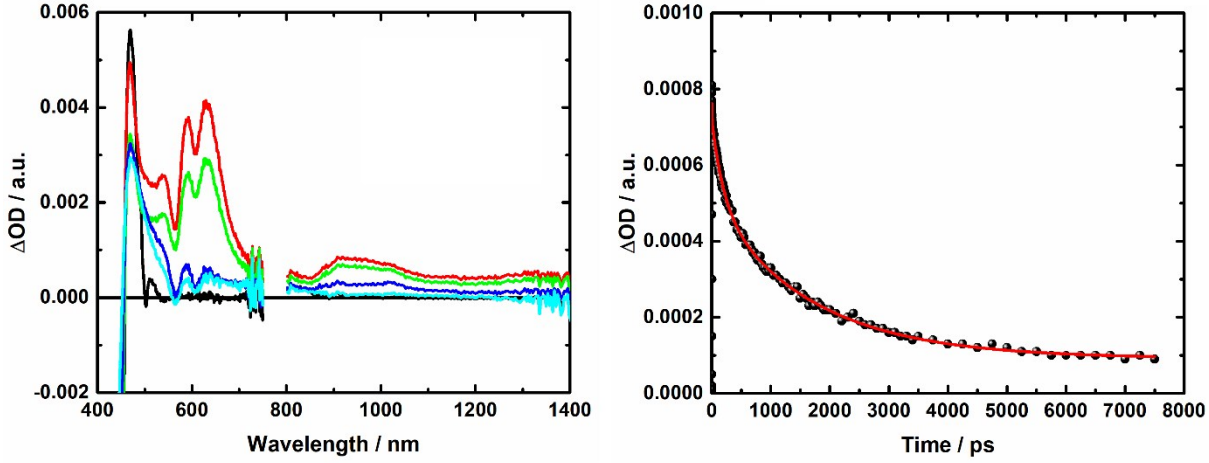

Fig. S20 Left: Femtosecond transient absorption spectra of **C_{60}-tpyr•[(ZnP)$_2$]$_2$** in argon saturated toluene containing 1 x 10^{-6} M **C_{60}-tpyr** and 2 x 10^{-6} M **(ZnP)$_2$** upon photoexcitation at 430 nm at different time delays, 1 ps (black), 10 ps (red), 100 ps (green), 1000 ps (blue) and 7500 ps (cyan). Right. Corresponding time absorption profile at 1014 nm. The solid line shows the triexponential fit of the transient absorption.

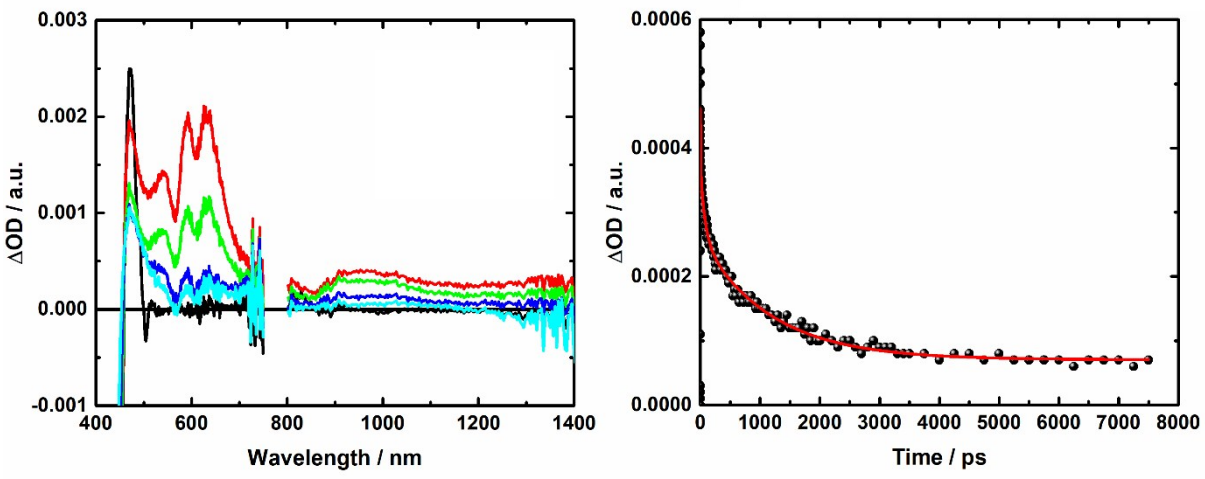

Fig. S21 Left: Femtosecond transient absorption spectra of **C_{60}-tpyr•[(ZnP)$_2$]$_2$** in argon saturated chlorobenzene containing 1 x 10^{-6} M **C_{60}-tpyr** and 2 x 10^{-6} M **(ZnP)$_2$** upon photoexcitation at 430 nm at different time delays, 1 ps (black), 10 ps (red), 100 ps (green), 1000 ps (blue) and 7500 ps (cyan). Right: Corresponding time absorption profile at 1014 nm. The solid line shows the triexponential fit of the transient absorption.

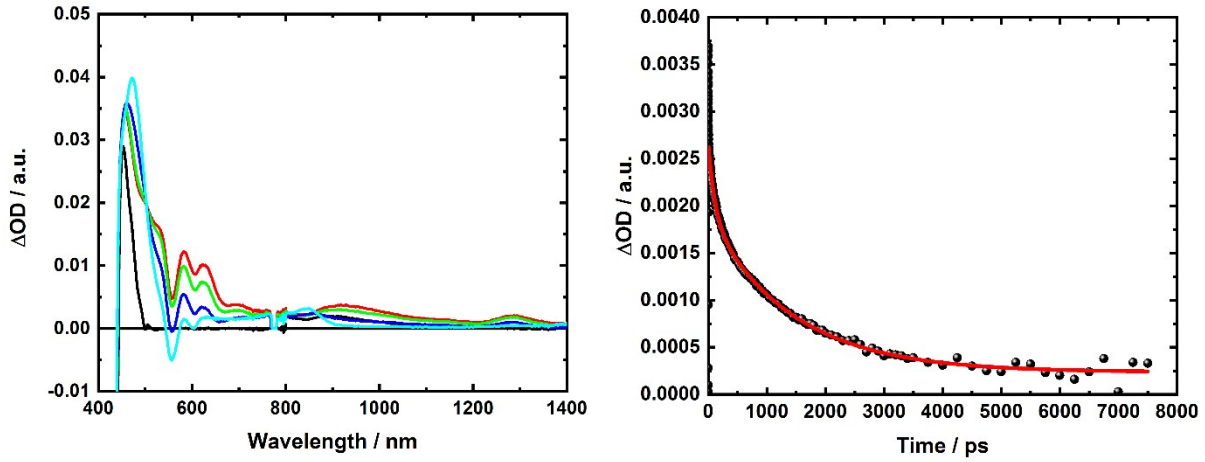

Fig. S22 Left: Femtosecond transient absorption spectra of **C_{60}-tpyr•(ZnP)$_4$** in argon saturated toluene containing 1 x 10^{-5} M **C_{60}-tpyr** and 4 x 10^{-5} M **ZnP** upon photoexcitation at 430 nm at different time delays, 1 ps (black), 10 ps (red), 100 ps (green), 1000 ps (blue) and 7500 ps (cyan). Right: Corresponding time absorption profile at 1014 nm. The solid line shows the biexponential fit of the transient absorption.

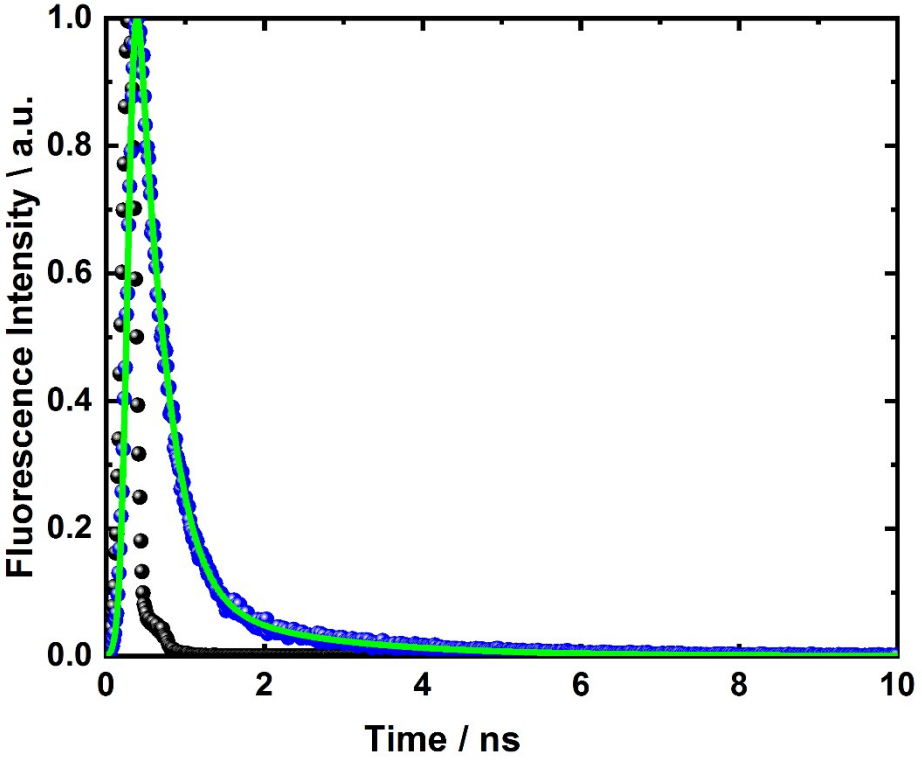

Fig. S23 Fluorescence time profiles of **C_{60}-tpyr•[(ZnP)$_2$]$_2$** (blue filled circles) in anisole at 600 nm upon photoexcitation at 430 nm. The instrument response function (IRF) is shown in black.